Table VII. Properties of Ion-Selective Membrane Electrodes

detection limit for Cu(II), M	10^{-6}
slope, mV/decade	28
response time, s	<10
selectivity coeff ($K^{pot}_{Cu,B}$)	
Ni(II)	10^{-1}
Co(II)	10^{-1}

macrocycles. The response characteristics of the electrodes in standard copper solutions are rather good, presenting near-Nernstian response, a low practical detection limit, and a short response time (Table VII).

Acknowledgment. This work was supported by the "Comisión Asesora de Investigación Científica y Técnica (CAICYT)", Spanish Government, through Grant No. MAT88-0179-C02-01 and by the "Fundación Ramón Areces", Spain.

Registry No. MO1, 59945-48-1; MO2, 59945-49-2; MO3, 52577-37-4; $Cu(MO1)Cl_2$, 132673-29-1; $Ni(MO1)Cl_2$, 132673-30-4; $Ni(MO1)(SCN)_2$, 132673-31-5; $Co(MO1)Cl_2$, 132673-32-6; $Co(MO1)(SCN)_2$, 132673-33-7; $Cu(MO2)Cl_2$, 132673-34-8; $Cu(MO2)Br_2$, 132698-27-2; $Ni(MO2)(SCN)_2$, 132673-35-9; $Co(MO2)(SCN)_2$, 132673-36-0; 2,6-bis(bromomethyl)pyridine, 7703-74-4; diethylene thiodiglycol, 2150-02-9; triethylene thiodiglycol, 14970-87-7; tetraethylene thiodiglycol, 2781-02-4; Cu, 7440-50-8.

Supplementary Material Available: Tables of anisotropic thermal parameters for both compounds (2 pages); tables of observed and calculated structure factors (21 pages). Ordering information is given on any current masthead page.

Contribution from the Laboratoire de Synthèse et d'Electrosynthèse Organometallique, Associé au CNRS (URA 33), Faculté des Sciences "Gabriel", Bd Gabriel, 21100 Dijon, France, Societe Elf France, Centre de Recherche de Solaize, Boite Postale n 22, 69360 St. Symphorien d'Ozon, France, and Department of Chemistry, University of Houston, Houston, Texas 77204-5641

Studies of Micellar Metalloporphyrins. Synthesis and Spectroscopic Characterization of $[(P)H_2]^+$ and $[(P)M^{II}]^+$, Where P = the Dianion of 5-(4-*N*-Hexadecylpyridiniumyl)-10,15,20-triphenylporphyrin Bromide and M = VO, Ni, or Cu

R. Guilard,*[1a] N. Senglet,[1a] Y. H. Liu,[1b] D. Sazou,[1b,c] E. Findsen,[1b] D. Faure,[1d] T. Des Courieres,[1d] and K. M. Kadish*[1b]

Received August 6, 1990

The synthesis and spectroscopic characterization of 5-(4-*N*-hexadecylpyridiniumyl)-10,15,20-triphenylporphyrin bromide (abbreviated as $[(hTriP)H_2]^+Br^-$) and its nickel, copper, and vanadyl metalated derivatives are reported. The investigated porphyrins are monomeric in neat ethanol or neat DMF, but the formation of micelles is demonstrated to occur in either ethanol–water or DMF–water mixtures containing 65–80% H_2O. UV–visible, NMR, and ESR spectroscopy and electron microscopy were used to characterize the porphyrins in both their monomeric and micellar forms. Electron microscopy of $[(hTriP)Ni]^+$ and $[(hTrip)Cu]^+$ shows that the diameter of the spherical micelles varies between 50 and 120 Å and also that these micelles decompose via further aggregation.

Introduction

Vanadium and nickel are two major metals found in crude oils. Neither metal is in an ionic form but is complexed by porphyrin macrocycles such as deoxophylloerythroetioporphyrin, etioporphyrin, and rhodoporphyrin.[2-6] A non-porphyrin fraction of nickel and vanadium may also be present,[7-9] but this has not been investigated in great detail.

The best method to quantitatively determine metalloporphyrins in crude oil involves UV–visible measurements at wavelengths of the porphyrin Soret band. This spectroscopic method is quite accurate in most cases, but low values are sometimes obtained for nonhomogeneous solutions, as recently demonstrated by an EXAFS study of asphaltenes.[10] The EXAFS spectra were strongly dominated by a pattern of vanadyl porphyrins (indicating a high concentration), but UV–visible spectra of the same solutions indicated that only trace amounts were present.

Differences between the EXAFS and UV–visible results can be related to the microheterogeneous nature of asphaltene solutions and indicate that more than one quantitative method is needed to characterize metalloporphyrins in heavy fractions of petroleum oils. The microheterogeneity of each asphaltene solution must also be examined in detail. In this regard, the most accurate method involves SAXS (small-angle X-ray scattering),[10-14] which gives an average size of the scattering particles in solution. SAXS requires the use of model compounds to determine the absolute size of aggregates in the asphaltene sample. The utilized model compound should contain a macrocyclic unit and should also form micelles in solution. The most ideal model compound would be a micellar metalloporphyrin.

A number of porphyrins and metalloporphyrins are known to aggregate in aqueous solutions,[15,16] organic solvents,[17] or mixed

(1) (a) University of Dijon. (b) University of Houston. (c) On leave from the University of Thessaloniki. (d) Societe Elf France.
(2) Barwise, A. J. G.; Whitehead, E. V. Symposium on Novel Methods of Metal and Heteroatom Removal. Presented at the 179th National Meeting of the American Chemical Society, Houston, TX, March 23–28, 1980.
(3) Fish, R. H.; Komlenic, J. J. *Anal. Chem.* **1984**, *56*, 510.
(4) Fookes, C. J. R. *J. Chem. Soc., Chem. Commun.* **1983**, 1472.
(5) Fookes, C. J. R. *J. Chem. Soc., Chem. Commun.* **1985**, 706.
(6) Ocampo, R.; Callot, H. J.; Albrecht, P. *J. Chem. Soc., Chem. Commun.* **1985**, 198.
(7) Reynolds, J. G.; Biggs, W. R.; Fetzer, J. C.; Gallegos, E. J.; Fish, R. H.; Komlenic, J. J.; Wines, B. K. *Collect. Colloq. Semin.* **1984**.
(8) Dickson, F. E.; Kunesh, C. J.; McGinnis, E. L.; Petrakis, L. *Anal. Chem.* **1972**, *44*, 978.
(9) Spencer, W. A.; Galobardes, J. F.; Curtis, M. A.; Rogers, L. B. *Sep. Sci. Technol.* **1982**, *17*, 797.
(10) Goulon, J. F.; Retournard, A.; Friant, P.; Goulon-Ginet, C.; Berthe, C.; Muller, J. F.; Poncet, J. L.; Guilard, R.; Escalier, J. C.; Neff, B. *J. Chem. Soc., Dalton Trans.* **1984**, 1095.
(11) Dickie, J. P.; Yen, T. F. *Anal. Chem.* **1967**, *39*, 1847.
(12) Pollack, S. S.; Yen, T. F. *Anal. Chem.* **1970**, *42*, 623.
(13) Kim, H.; Long, R. B. *Ind. Eng. Chem. Fundam.* **1979**, *18*, 60.
(14) Ho, B.; Briggs, D. E. *Colloids Surf.* **1982**, *4*, 285.
(15) (a) Takami, A.; Mataga, N. *J. Phys. Chem.* **1987**, *4*, 285. (b) White, W. I. In *The Porphyrins*; Dolphin, E., Ed.; Academic Press: New York, 1978; Vol. 5, Chapter 7. (c) Satterlee, J. D.; Shellnutt, J. A. *J. Phys. Chem.* **1984**, *88*, 5487. (d) Chadrashekar, T. K.; van Willigen, H.; Ebsersole, M. H. *J. Phys. Chem.* **1984**, *88*, 4326. (e) Pasternack, R. F.; Gibbs, E.; Gaudemer, A.; Antebi, A.; Bassner, S.; DePoy, L.; Turner, D. H.; Williams, A.; Laplace, F.; Lansard, M. H.; Merriene, C.; Perree-Fauvet, M. *J. Am. Chem. Soc.* **1985**, *107*, 8179. (f) Kano, K.; Miyake, T.; Uomoto, K.; Sato, T.; Ogawa, T.; Hashimoto, S. *Chem. Lett.* **1983**, 1867. (g) Kano, K.; Nakajima, T.; Takei, M.; Hashimoto S. *Bull Chem. Soc. Jpn.* **1987**, *60*, 1281.
(16) Fuhrhop, J.-H.; Baccouche, M. *Liebigs Ann. Chem.* **1976**, 2058.
(17) Yamamura, T. *Chem. Lett.* **1977**, 773.

0020-1669/91/1330-1898$02.50/0

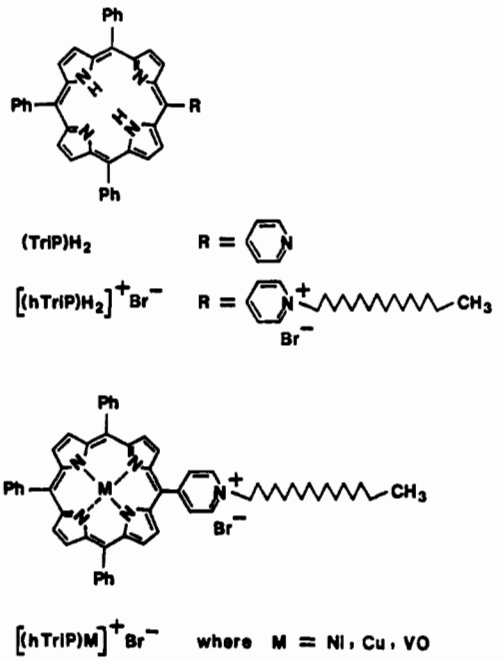

Figure 1. Structures of investigated metalloporphyrins.

water–organic solvent mixtures.[18] The formation of porphyrin micelles from $[(DTriP)Cu]^+Br^-$, where DTriP = the dianion of 5-(4-*N*-dodecylpyridiniumyl)-10,15,20-triphenylporphyrin bromide, has also been reported to occur in ethanol–water mixtures[18] and was accompanied by a decreased intensity of the porphyrin Soret band as well as by changes in the Cu(II) ESR spectra with respect to values obtained for the monomeric species in neat EtOH. A decreased Soret band intensity has also been noted for vanadyl and nickel porphyrins in asphaltene solutions, and this would account for the incorrectly low metal concentrations that are sometimes obtained by UV–visible spectroscopic analysis.

It is clear that porphyrins that can form micelles should be examined in greater detail, both in their monomeric form and under solution conditions where micelles are generated. This is done in the present paper, which reports the synthesis and spectroscopic characterization of 5-(4-*N*-hexadecylpyridiniumyl)-10,15,20-triphenylporphyrin bromide (abbreviated as $[(hTriP)H_2]^+Br^-$) and its nickel, copper, and vanadyl metalated derivatives. Structures of these compounds are given in Figure 1. UV–visible, ^1H NMR, and ESR spectroscopy was used to characterize each complex in both protic and aprotic nonaqueous media where only monomers are present. Micelles are formed in ethanol–water or DMF–water mixtures, and these were characterized by various methods under several experimental conditions.

Experimental Section

Materials. Methylene chloride (CH_2Cl_2) was purchased from J. T. Baker Chemical Co. and purified by distillation over P_2O_5 just prior to use. Pyridine (py) obtained from Mallinckrodt was twice distilled from calcium hydride. Spectroscopic grade dimethylformamide (DMF), purchased from J. T. Baker, was twice distilled over molecular sieves under reduced pressure. Absolute ethanol (EtOH) was purchased from Midwest Solvents Co. and used as received. Deionized water was distilled over $KMnO_4$ prior to use.

All syntheses were carried out in the open air. N-alkylation of $(TriP)H_2$ to give $[(hTriP)H_2]^+$ and metalation by copper ion to give $[(hTriP)Cu]^+$ were carried out as described for $[(DTriP)H_2]^+$.[18] The metalation of $[(hTriP)H_2]^+$ by nickel or vanadyl ions to give $[(hTriP)Ni]^+$ and $[(hTriP)VO]^+$ is described in the following sections.

5-(4-Pyridyl)-10,15,20-triphenylporphyrin, $(Trip)H_2$. The synthesis of 5-(4-pyridyl)-10,15,20-triphenylporphyrin, $(TriP)H_2$, is described in the literature[19,20] and was improved upon in this present study using a modification suggested by Lavallee.[21] In this modified method, a mixture containing 14 mL of benzaldehyde (0.138 mol), 6 mL of 4-pyridinecarboxaldehyde (0.063 mol), and 12.5 mL of distilled pyrrole (0.18 mol) was added dropwise to 500 mL of refluxing propionic acid. The reaction mixture was then refluxed with stirring for 1 h 30 min. After the mixture was cooled to 90 °C, 350 mL of diethylene glycol was added to the solution and the mixture slowly cooled in ice-water and allowed to stand overnight in the refrigerator. Filtration and washing with methanol gave 6.25 g of crude product. The solid was dissolved in hot chloroform and chromatographed with SiO_2 by eluting first with methylene chloride (to eliminate the free base; 2.43 g) and then with a 9:1 methylene chloride–methanol mixture. Removal of the solvent, washing with heptane, and drying gave 1.8 g of the final product (4.6% yield).

5-(4-*N*-Hexadecylpyridiniumyl)-10,15,20-triphenylporphyrin Bromide, $[(hTriP)H_2]^+Br^-$. A 1.63-mmol sample of $(TriP)H_2$ was added to 5 mL of 1-bromohexadecane (16.30 mmol) in 1 L of DMF and the mixture then refluxed for 3 h. After evaporation of the solvent, the residual solid was washed with ether and filtered out. Purification of the solid by chromatography on an aluminum oxide column (eluents CH_2Cl_2 and then CH_2Cl_2–CH_3OH (9:1)) gave 810 mg (54% yield) of $[(hTriP)H_2]Br^-$.

Copper 5-(4-*N*-Hexadecylpyridiniumyl)-10,15,20-triphenylporphyrin Bromide. A 1.09-mmol sample of $[(hTriP)H_2]^+Br^-$ was added to 1.40 L of MeOH containing 1.12 mmol of $CuBr_2$ and the mixture refluxed for 1 h. Purification by chromatography on an aluminum oxide column gave 810 mg (76% yield) of $[(hTriP)Cu]^+Br^-$. Anal. Calc for $[(hTriP)Cu]^+Br^-$, $C_{59}H_{60}N_5BrCu$: C, 72.13; H, 6.11; N, 7.13; Br, 8.15; Cu, 6.47. Found: C, 71.17; H, 6.02; N, 6.76; Br, 8.83; Cu, 6.57.

Nickel 5-(4-*N*-Hexadecylpyridiniumyl)-10,15,20-triphenylporphyrin Bromide. A 0.49-mmol amount of $[(hTriP)H_2]^+Br^-$ was added to 1.25 L of DMF containing 0.84 mmol of $NiCl_2 \cdot 6H_2O$ and the mixture refluxed for 1 h 30 min. Purification by chromatography on an aluminum oxide column gave 360 mg (75% yield) of $[(hTriP)Ni]^+Br^-$. Anal. Calc for $[(hTriP)Ni]^+Br^- \cdot H_2O$, $C_{59}H_{60}N_5BrNi \cdot H_2O$: C, 71.15; H, 6.23; N, 7.05; Br, 8.04; Ni, 5.9. Found: C, 71.36; H, 5.72; N, 7.28; Br, 8.08; Ni, 5.94.

Vanadyl 5-(4-*N*-Hexadecylpyridiniumyl)-10,15,20-triphenylporphyrin Bromide. A 0.90-mmol amount of $[(hTriP)H_2]^+Br^-$ was added to 180 mL of benzonitrile containing 5.08 mmol of VCl_3 and the mixture refluxed for 1 h. Purification by chromatography on an aluminum oxide column gave 410 mg (46% yield) of $[(hTriP)VO]^+Br^-$. Anal. Calc for $[(hTriP)VO]^+Br^-$, $C_{59}H_{60}N_5BrVO$: C, 71.88; H, 6.09; N, 7.10; V, 5.18. Found: C, 71.58; H, 6.40; N, 7.33; V, 5.88.

Physical Measurements. Elemental analyses were performed by Schwarzkopf Microanalytical Laboratory. Electronic absorption spectra were performed on a Perkin-Elmer 559 spectrophotometer or an IBM 9430 UV–visible spectrophotometer. ^1H NMR spectra were recorded on a Bruker WM 400 spectrometer. Spectra were measured in a 0.5 mL solution of $CDCl_3$ with tetramethylsilane as an internal reference. ESR spectra were recorded on an IBM Model ER-100D electron spin resonance system or a Bruker ESP 300 spectrometer interfaced with an Aspect 2000/3000 computer. Measurements were made at 298 K or at 100 K by using a variable-temperature unit. An ESR simulation of each spectrum was also carried out. Electron microscopy was performed with a JEOL JEM 100C microscope equipped with a goniometric table (±20° rotation) of 100 kV voltage and a pole-piece having an interferential resolution of 1.4 Å.

All samples were prepared by completely dissolving the porphyrins in EtOH or DMF, after which water was added to obtain the given solution. Solutions were sonicated for 1 min immediately after the addition of water. Measurements of time-dependent UV–visible and ESR spectra were taken with the initial time being the beginning of sonification. Samples for ESR measurements were prepared by first transferring the solution to an ESR tube, after which it was frozen in liquid nitrogen.

Results and Discussion

^1H NMR Characterization. NMR spectral data for $(TriP)H_2$, $[(hTriP)H_2]^+$, and $[(hTriP)Ni]^+$ in $CDCl_3$ are summarized in Table I. The $(TriP)H_2$ complex has resonances at 8.87 and −2.8 ppm, which are assigned to the pyrrole and NH protons. The phenyl and pyridyl meso substituents of the free-base porphyrin have signals located between 7.78 and 9.04 ppm (see Table I).

The ^1H NMR spectrum of the N-substituted complex, $[(hTriP)H_2]^+$, is uncomplicated and has resonances attributed to the alkyl chain at 0.86 (methyl protons), 1.24 (26 methylenic

(18) Tajima, K.; Ishikawa, Y.; Mukai, K.; Ishizu, K.; Sakurai, H. *Bull. Chem. Soc. Jpn.* **1984**, *57*, 3587.
(19) Shamim, A.; Hambright, P.; Williams, R. F. X. *Inorg. Nucl. Chem. Lett.* **1979**, *15*, 243.
(20) Williams, G. N.; Williams, R. F. X.; Lewis, A.; Hambright, P. *J. Inorg. Nucl. Chem.* **1979**, *41*, 41.
(21) Lavallee, D. K. Private communication.

Table I. ^{1}H NMR Data for $(TriP)H_2$, $[(hTriP)H_2]^+$, and $[(hTriP)Ni]^+$ [a,b]

				protons of R^1		protons of R^2			protons of R^3		
compd	R^1	R^2	R^3	m/*i*[c]	δ	m/*i*		δ	m/*i*		δ
$(TriP)H_2$	H	C_6H_5	C_5H_4N	M/8	8.87	*o*-H	M/6	8.2	α-H	d/2	9.04
						o'-H			α'-H		
									β-H		
						m-H				d/2	8.8
						m'-H	M/9	7.78	β'-H		
						p-H					
$[(hTriP)H_2]^+$	H	C_6H_5	$C_5H_4N(CH_2)_{15}CH_3$	d/2	8.81	*o*-H			α-H		
				q/4			M/6	8.16		d/2	9.71
					8.85	*o'*-H			α'-H		
				d/2	8.96						
									β-H		
						m-H				d/2	8.77
						m'-H	M/9	7.75	β'-H		
						p-H					
									α-CH_2[d]	t/2	5.32
									β-CH_2[d]	M/2	2.35
									CH_2	M/26	1.24
									CH_3	t/3	0.86
$[(hTriP)Ni]^+$	H	C_6H_5	$C_5H_4N(CH_2)_{15}CH_3$	d/2	8.63	*o*-H			α-H		
				q/4			M/6	7.94		d/2	9.72
					8.75	*o'*-H			α'-H		
				d/2	8.83						
									β-H		
						m-H				d/2	8.58
						m'-H	M/9	7.67	β'-H		
						p-H					
									α-CH_2	t/2	5.32
									β-CH_2	M/2	2.31
									CH_2	M/26	1.24
									CH_3	t/3	0.87

[a] Spectra recorded at 21 °C in $CDCl_3$ with $SiMe_4$ as internal reference; chemical shifts downfield from $SiMe_4$ are defined as positive. [b] R^1 = pyrrole protons, R^2 = unsubstituted phenyl group protons, and R^3 = N-alkylated phenyl group protons. [c] Legend: m = multiplicity; *i* = intensity; d = doublet; t = triplet; q = quartet; M = multiplet. [d] α and β position of the methylenes in relation to the pyridinium nitrogen.

Table II. UV–Visible Data for $(TriP)H_2$, $[(hTriP)H_2]^+$, and $[(hTriP)M]^+$ in CH_2Cl_2

compd[a]	λ_{max} ($10^{-3}\epsilon$[b])				
$(TriP)H_2$	417 (455), 480 (1.6)	514 (17.2)	549 (5.9)	589 (4.7)	644 (3.1)
$[(hTriP)H_2]^+$	419 (145)	520 (6.8)	565 (5.3)	590 (4.6)	653 (4.1)
$[(hTriP)Ni]^+$	411 (111)	533 (9.1)		574 (sh)[c]	
$[(hTriP)Cu]^+$	415 (151)	545 (11.1)		591 (4.7)	
$[(hTriP)VO]^+$	424 (279)	549 (17.5)		588 (3.2)	

[a] Concentration between 2×10^{-5} and 7×10^{-5} M. [b] λ in nm; ϵ in M^{-1} cm^{-1}. [c] sh = shoulder.

protons), 2.35 (β-CH_2), and 5.32 ppm (α-CH_2). The large deshielding of the α-CH_2 protons can be explained by the proximity of the nitrogen atom to the pyridinium moiety.

The alkyl chain of $[(hTriP)H_2]^+$ or $[(hTriP)Ni]^+$ does not induce significant shifts in the meso substituent resonances except for those of the pyridinium α protons. $[(hTriP)Ni]^+$ exhibits features typical of a diamagnetic four-coordinate Ni(II) porphyrin, and these features contrast with those of five- and six-coordinate Ni(II) derivatives, all of which are paramagnetic.[22a] The metalation of $[(hTriP)H_2]^+$ by Ni(II) induces a shielding of all protons of the macrocycle (pyrrole protons, $0.1 < \Delta\delta < 0.18$ ppm; phenyl protons, 0.22 ppm for *o*-H and 0.08 ppm for *m*- and *p*-H; pyridyl β protons, 0.19 ppm) except for those of the $(CH_2)_{15}$–CH_3 alkyl chain, which are at a large distance from the Ni(II) center and are unaffected.

UV-Visible Spectroscopy. UV–visible data for $(TriP)H_2$, $[(hTriP)H_2]^+$, and $[(hTriP)M]^+$ where M = Ni, Cu, or VO are summarized in Table II. Each metalated complex exhibits a normal electronic absorption spectra[22b] and has Q and B bands that are red shifted in the order Ni(II) < Cu(II) < $V^{IV}O$. There is a large decrease in the apparent molar absorptivity of the complexes after N-alkylation of $(TriP)H_2$ to give $[(hTriP)H_2]^+$.

The apparent molar absorptivities of $[(hTriP)Ni]^+$ or $[(hTriP)Cu]^+$ differ significantly between neat ethanol and ethanol–water mixtures or between neat DMF and DMF–H_2O mixtures. A solvent effect on the UV–vis spectra is also observed for the free base and VO^{2+} derivatives, and this is shown in Figure 2 for $[(hTriP)M]^+$, where M = Ni, Cu, or VO. The Soret band decreases to a minimum in solutions containing 60–80% H_2O (see Table III for 70% H_2O). There is a large decrease in the absorbance of $[(hTriP)Ni]^+$ or $[(hTriP)Cu]^+$ in EtOH–H_2O mixtures as well as a small red shift in the spectrum compared to that of the same porphyrin in neat EtOH. In contrast, $[(hTriP)VO]^+$ undergoes a blue shift in the spectrum, and the intensities of the Soret and Q bands change only slightly upon going from EtOH to an EtOH–H_2O mixture with 70% H_2O. This is shown in Figure 2 (bottom) and can be accounted for by axial coordination of EtOH or H_2O.

Vanadyl porphyrins of the type (P)VO are able to bind an additional axial ligand to form six-coordinate (P)VO(L) species.[23,24] A coordination of $[(hTriP)VO]^+$ by DMF was ascertained

(22) (a) LaMar, G. N.; Walker, F. A. In *The Porphyrins*; Dolphin, D., Ed.; Academic: New York, 1978; Vol. IV, Chapter 2 and references therein. (b) Gouterman, M. In *The Porphyrins*; Dolphin, D., Ed.; Academic: New York, 1978; Vol. III, Chapter 1 and references therein.

(23) Bencosme, S.; Romero, C.; Simoni, S. *Inorg. Chem.* **1985**, *24*, 1603.

(24) Walker, F. A.; Hui, E.; Walker, J. M. *J. Am. Chem. Soc.* **1975**, *97*, 2390.

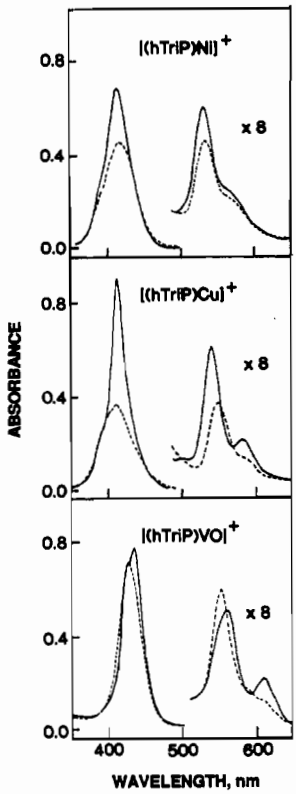

Figure 2. Electronic absorption spectra of 5.23×10^{-5} M $[(hTriP)Ni]^+$, 4.45×10^{-5} M $[(hTriP)Cu]^+$, and 3.83×10^{-5} M $[(hTriP)VO]^+$ in EtOH (—) and an EtOH–H_2O mixture containing 70% H_2O (---).

Table III. Maximum Absorbance Wavelength (λ_{max}) and Corresponding Molar Absorptivities (ϵ) of $[(hTriP)M]^+$ Complexes

compd	λ_{max} ($10^{-3}\epsilon$)[a]			
	EtOH		EtOH–H_2O (3:7)	
$[(hTriP)Ni]^+$[b]	413 (132)	529 (11.5)	416 (87.1)	532 (8.7)
$[(hTriP)Cu]^+$[c]	413 (180)	540 (12.6)	413 (72.0)	549 (7.6)
$[(hTriP)VO]^+$[d]	434 (201)	562 (13.1)	426 (185.0)	551 (19.3)

[a] λ in nm; ϵ in M^{-1} cm^{-1}. Values of ϵ in the EtOH–H_2O mixture are only apparent values and depend upon both the porphyrin concentration and the specific EtOH:H_2O ratio. [b] Concentration = 5.23×10^{-5} M. [c] Concentration = 4.45×10^{-5} M. [d] Concentration = 3.83×10^{-5} M.

in the present study by monitoring the UV–visible spectrum of the complex in solutions with different CH_2Cl_2:DMF ratios. The resulting spectral data are shown in Figure 3, which graphically illustrates the increase in Soret band absorption at 434 nm and the simultaneous decrease in the 424 nm absorption band as the concentration of DMF is increased. Similar changes have been reported for other vanadyl porphyrins in CH_2Cl_2–DMF mixtures[25] and were interpreted in terms of DMF coordination. The Soret band of $[(hTriP)VO]^+$ is located at 424 nm in CH_2Cl_2 and 434 nm in EtOH (see Tables II and III), and this shift in λ_{max} also suggests a coordination of EtOH to the complex. On the other hand, the shifts in absorption maxima from 434 to 426 nm and 562 to 551 nm upon going from neat EtOH to an EtOH–H_2O mixture with 70% H_2O (Table III) is consistent with dissociation of EtOH from $[(hTriP)VO(EtOH)]^+$ upon addition of water.

Decreased UV–visible absorptions for porphyrins with similar structures were reported to occur in EtOH–H_2O mixtures,[18] but no information was provided as to the stability of the resulting complexes. The species formed from $[(hTriP)M]^+$ in solutions containing 60–80% H_2O are unstable, and this is illustrated by the data in Figure 4a,b, which show the time-dependent spectral

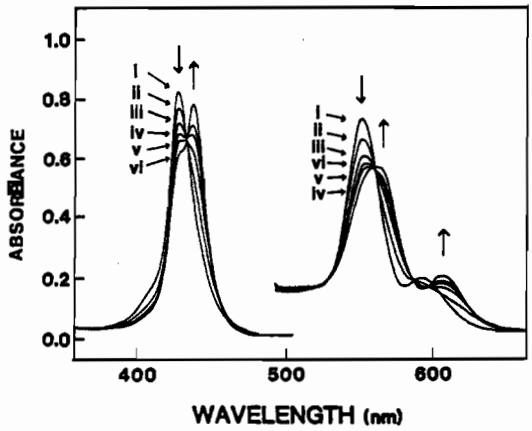

Figure 3. Electronic absorption spectra of 2.21×10^{-5} M $[(hTriP)VO]^+$ in solutions containing the following CH_2Cl_2:DMF ratios: (i) 10:0; (ii) 8:2; (iii) 6:4; (iv) 5:5; (v) 4:6; (vi) 2:8.

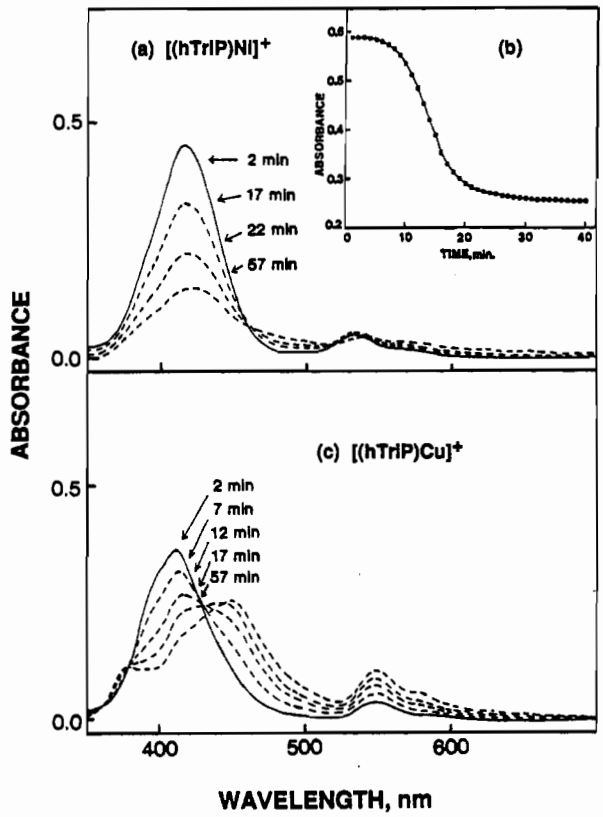

Figure 4. (a) UV–visible spectra of 5.23×10^{-5} M $[(hTriP)Ni]^+$ in an EtOH–H_2O mixture with 70% H_2O at various times after solution preparation. (b) Time-dependent changes in the 416-nm band of 5.11×10^{-5} M $[(hTriP)Ni]^+$ in EtOH–H_2O with 70% H_2O. (c) UV–visible spectra of 4.45×10^{-5} M $[(hTriP)Cu]^+$ in an EtOH–H_2O mixture with 70% H_2O at various times after solution preparation.

changes that occur for $[(hTriP)Ni]^+$ and $[(hTriP)Cu]^+$ after preparation in an ethanol–water mixture with 70% H_2O.

The intensity of the 416-nm Soret band of $[(hTriP)Ni]^+$ is plotted as a function of time in Figure 4b. The absorbance is constant for 4 min after solution preparation but then begins to decrease and reaches a minimum after 30–40 min, as the solution becomes turbid. These results indicate that the species in solution is stable only for very short time periods after which precipitation begins. A decrease of absorbance does not occur with time for $[(hTriP)Ni]^+$ in mixed DMF–H_2O or EtOH–H_2O solvents with greater than 80% H_2O, and no precipitation of the porphyrin is observed under these solution conditions.

The Soret band absorbances of $[(hTriP)Ni]^+$ and $[(hTriP)Cu]^+$ were also recorded as a function of time and H_2O content in solutions with different EtOH:H_2O or DMF:H_2O ratios. These

(25) Kadish, K. M.; Sazou, D.; Araullo, C.; Liu, Y. M.; Saioabi, A.; Ferhat, M.; Guilard, R. *Inorg. Chem.* **1988**, *27*, 2313.

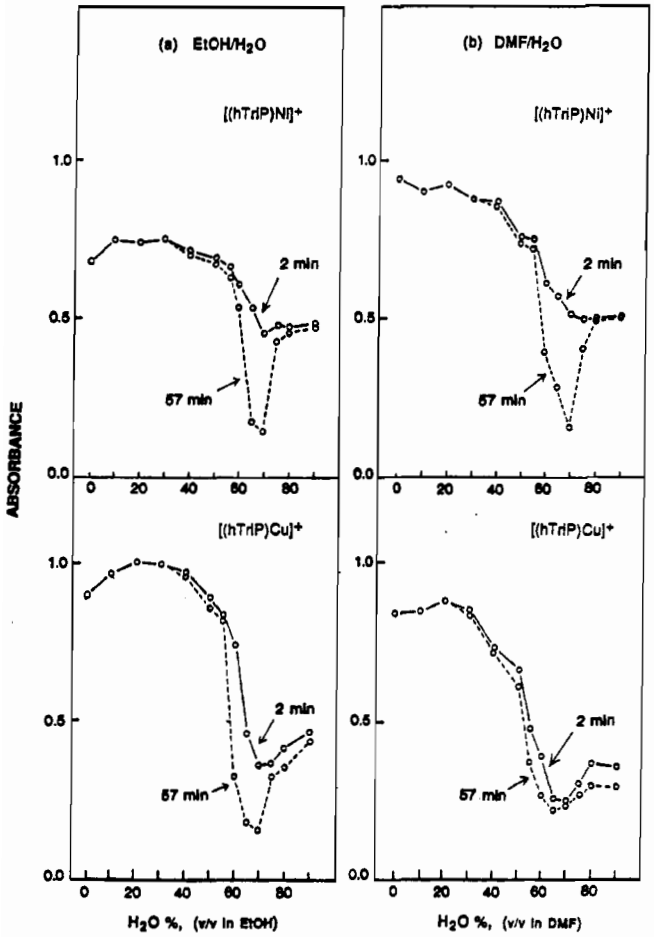

Figure 5. Dependence of Soret band absorbance on H_2O content for solutions containing (a) 5.23×10^{-5} M $[(hTriP)Ni]^+$ and 4.45×10^{-5} M $[(hTriP)Cu]^+$ in EtOH–H_2O solutions and (b) 5.24×10^{-5} M $[(hTriP)Ni]^+$ and 4.32×10^{-5} M $[(hTriP)Cu]^+$ in DMF–H_2O solutions. Data were taken 2 min (—) and 57 min (---) after solution preparation.

results are shown in Figure 5. The absorbances of the Ni(II) complex do not change with time in solutions containing 0–30% H_2O and decrease only slightly in solutions containing 40–50% H_2O. This contrasts with solutions containing 50–65% H_2O, where a substantial decrease in the absorbance with time is noted. A minimum Soret band absorbance is recorded for $[(hTriP)Ni]^+$ in solutions containing ~70% H_2O, and these solutions are turbid due to precipitation of the porphyrin. Finally, a clear solution is observed in solutions with 80–90% H_2O and no solid formation is observed under these conditions.

The $[(hTriP)Cu]^+$ complex undergoes similar changes with time and water content, and the initial Soret band absorbance is much lower in solvents containing 70% H_2O than in solvents with 80–90% H_2O (see Figure 5a,b). However, $[(hTriP)Cu]^+$ in DMF–H_2O mixtures has similar absorptions after 2 and 57 min in all solutions containing 65–90% H_2O. Also, the absorbance decrease for $[(hTrip)Cu]^+$ with time is smaller than that for $[(hTrip)Ni]^+$ with time under the same solution conditions, thus indicating that the copper porphyrin micelles are less stable than the nickel porphyrin micelles in the presence of 65–75% H_2O.

A decrease of absorbance has been reported for the water-soluble porphyrin (TPPC)Pd (TPPC is the tetrakis(carboxyphenyl)porphyrin ligand) with increasing H_2O content in DMF–H_2O mixtures, and this was attributed to aggregation.[26] A slow precipitation of (TPPC)Pd was also reported to occur in DMF–H_2O mixtures containing larger than 60% H_2O. The compounds investigated in this present study show a continuous decrease of absorbance as the water content is increased from 40 to 75%, and these solutions precipitate when the H_2O content is between 65

(26) Assour, J. M. *J. Chem. Phys.* **1965**, *43*, 2477.

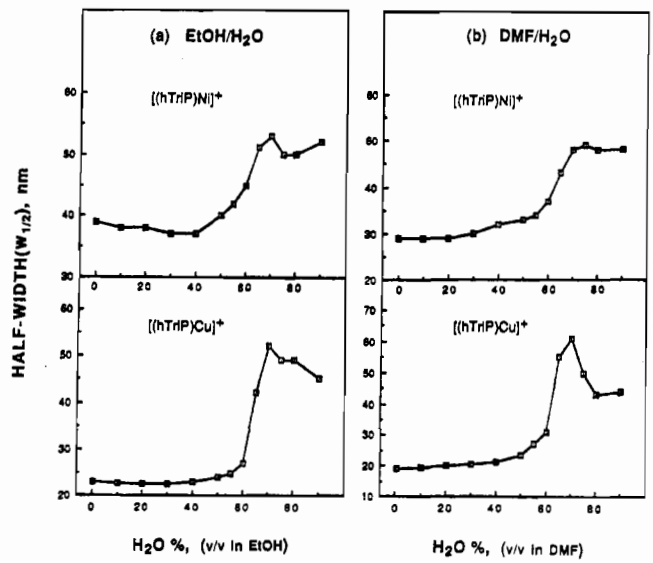

Figure 6. Half-width ($w_{1/2}$) of porphyrin Soret band of (a) 5.23×10^{-5} M $[(hTriP)Ni]^+$ and 4.45×10^{-5} M $[(hTriP)Cu]^+$ in EtOH–H_2O solutions and (b) 5.24×10^{-5} M $[(hTriP)Ni]^+$ and 4.32×10^{-5} M $[(hTriP)Cu]^+$ in DMF–H_2O solutions. All measurements were taken 2 min after mixing.

and 75%. This contrasts with results for solutions containing >80% H_2O, which have higher absorbances that do not change with time, as is the case for $[(hTriP)Ni]^+$. Clearly, (TPPC)Pd and $[(hTriP)M]^+$ show a different type of aggregation phenomenum and this is attributed to micellization for the latter series of complexes.

Determination of Critical Micelle Concentration (Cmc). The half-width of the porphyrin Soret band ($w_{1/2}$) is a parameter that has been related to the degree of aggregation.[27] This parameter varies between 36 and 50 nm for the investigated compounds and is plotted in Figure 6 vs water content for $[(hTriP)Ni]^+$ and $[(hTriP)Cu]^+$ in solutions with different EtOH:H_2O or DMF:H_2O ratios. The magnitude of $w_{1/2}$ increases substantially with H_2O content for solutions with >50–60% H_2O and is maximum in solutions of 70% H_2O. The cmc of surfactants will also depend upon the solution composition in mixed-solvent systems and reaches a minimum for solutions with a given aqueous–organic solvent ratio.[28-30]

The cmc of a given surfactant solution is typically obtained by monitoring a specific physical property of the solution (such as conductance or turbidity) as a function of the monomeric species concentration. The specific concentration where the measured physical property deviates from linearity is then assigned as the cmc.

The absorbances of $[(hTriP)Ni]^+$ in EtOH–H_2O mixtures with 70% H_2O increase with porphyrin concentration up to $\sim 2 \times 10^{-5}$ M but deviate from linearity at porphyrin concentrations higher than 4×10^{-5} M. The deviation begins to occur at a concentration of about 3×10^{-5} M, and this value can be assigned as the cmc. The UV–visible data suggest that metastable micelles of $[(hTrip)Ni]^+$ and $[(hTrip)Cu]^+$ are formed within 2 min after solution preparation but the two porphyrins then begin to precipitate after standing for 3–5 min. In order to monitor the degree of precipitation, the absorbance of $[(hTriP)Ni]^+$ was recorded every 10 min, and these data are shown in Figure 7. As seen in the figure, the absorbance of $[(hTriP)Ni]^+$ is proportioned to concentration up to $\sim 2.0 \times 10^{-5}$ M, at which point a deviation from Beer's law behavior occurs. This deviation becomes larger at longer times and reaches a maximum for measurements made 32 min after solution preparation. At this point, there is no longer

(27) Cellarius, R. A.; Mauzerall, D. *Biochem. Biophys. Acta* **1966**, *112*, 235.
(28) Flockhart, B. D. *J. Colloid Sci.* **1959**, *12*, 557.
(29) Suzuki, H. *Bull. Chem. Soc. Jpn.* **1976**, *49*, 1470.
(30) Cipiciani, A.; Onori, G. *Chem. Phys. Lett.* **1988**, *143*, 505.

Table IV. ESR Data for $[(hTriP)Cu]^+$ and $[(hTriP)VO]^+$ in Various Solvents

compd	solvent	A_{iso},[a] G	g_{iso}[a]	$A_\parallel$,[b] G	$g_\parallel$[b]	$A_\perp$,[b] G	$g_\perp$[b]
$[(hTriP)Cu]^+$	CH_2Cl_2	92.00	2.1030				
	EtOH	107.40	2.0791	199.00	2.1989	61.60	2.0193
$[(hTriP)VO]^+$	CH_2Cl_2	96.33	1.9796	170.71	1.9662	59.29	1.9846
	DMF	91.67	1.9811	171.71	1.9659	60.14	1.9854
	EtOH	86.80	1.9872	170.57	1.9659	59.71	1.9861
	EtOH–H_2O			170.57	1.9659	59.71	1.9861

[a] 298 K. [b] 100 K.

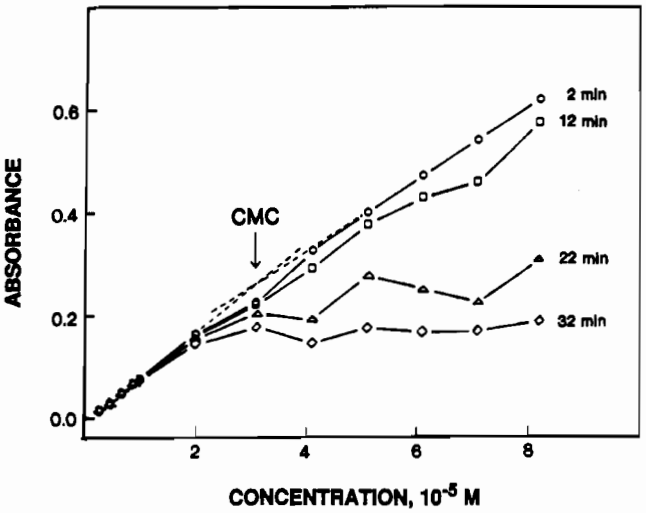

Figure 7. Absorption maxima for the 416-nm band of $[(hTriP)Ni]^+$ in an EtOH–H_2O mixture with 70% H_2O at various times after solution preparation.

an increase in absorbance with increase in the porphyrin concentration.

The limiting absorbance in Figure 7 corresponds to that of a monomeric species which has not precipitated out of solution, and the point at which deviation from Beer's law begins to occur (2.0×10^{-5} M) can then be regarded as a cmc. The difference between the measured cmc of 3.0×10^{-5} M (obtained after 2 min) and the smaller value of 2.0×10^{-5} M (obtained after 32 min) is attributed to precipitation, which shifts the equilibrium to the right as shown:

$$\text{monomers} \rightleftarrows \text{micelles} \rightleftarrows \text{precipitates}$$

ESR Characterization. ESR spectra of $[(hTriP)Cu]^+$ in solutions with different EtOH:H_2O ratios are shown in Figure 8, and the data in both neat EtOH and an EtOH–H_2O mixture with 80% H_2O are summarized in Table IV. The signal in pure EtOH is typical of monomeric Cu(II).[31,32] The g factor and hyperfine splitting constants in 50% H_2O (Figure 8b) are the same as in neat EtOH (Figure 8a), and this suggests that the porphyrin remains monomeric in 50% H_2O. However, when the H_2O content is increased to 60% (Figure 8c), the intensity of the nitrogen hyperfine coupling decreases and a broad signal appears at $g = 2.006$. There is no hyperfine splitting in solutions containing 65% H_2O (Figure 8d), and only one broad signal is observed.

The spectrum in Figure 8d is similar to spectra reported for dimeric,[33-35] highly aggregated,[36] or micellized[18] copper porphyrins. It is also similar to the signal of Cu(II) complexed with an aza crown ether surfactant.[37] This broad signal can result from a spin–spin interaction of the adjacent copper(II) ions in the micellized form. Moreover, there is not a signal located at $g \approx 4$, which would be expected to occur for a transition of the triplet state formed by coupling of the copper(II) ions of a dimer.[34]

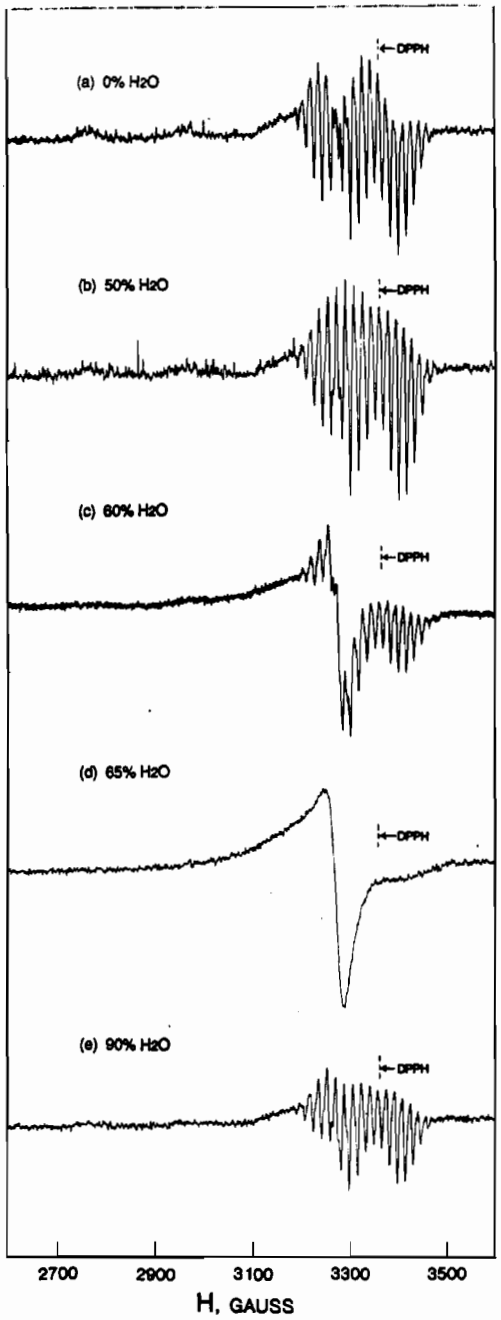

Figure 8. ESR spectra of 5.3×10^{-5} M $[(hTriP)Cu]^+$ in an EtOH–H_2O mixture containing the following % H_2O: (a) 0; (b) 50; (c) 60; (d) 65; (e) 90. All measurements were made 2 min after solution preparation.

(31) Subramanian, J. In *Porphyrins and Metalloporphyrins*; Smith, K. M., Ed.; Elsevier: Amsterdam, 1975; p 555.
(32) Manoharan, P. T.; Rogers, M. T. In *Electron Spin Resonance of Metal Complexes*; Yen, T. F., Ed.; Plenum: New York, 1969; p 143.
(33) De Bolfo, J. A.; Smith, T. D.; Boas, J. E.; Pilbrow, J. R. *J. Chem. Soc., Dalton Trans.* **1975**, 1523.
(34) Boyd, P. D. W.; Smith, T. D. *J. Chem. Soc., Dalton Trans.* **1972**, 839.
(35) Boyd, P. D. W.; Smith, T. D.; Price, J. H.; Pilbrow, J. R. *J. Chem. Phys.* **1972**, *56*, 1253.
(36) Konishi, S.; Hoshimo, M.; Imamura, M. *Chem. Phys. Lett.* **1983**, *94*, 267.
(37) Kunitake, T.; Ishikawa, Y.; Shimoumura, M. *J. Am. Chem. Soc.* **1986**, *108*, 327.

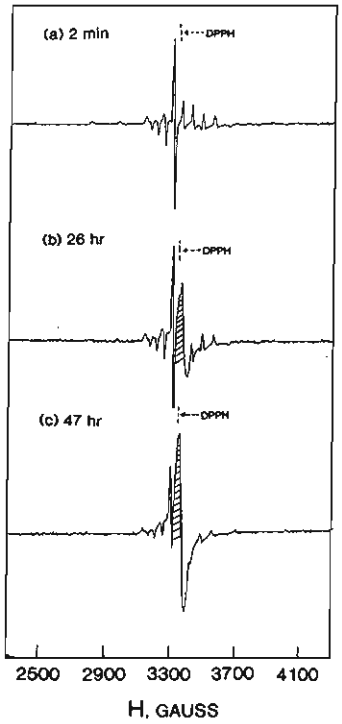

Figure 9. Time-dependent ESR spectra of 5.9×10^{-5} M $[(hTriP)VO]^+$ recorded at 134 K in an EtOH–H_2O solution containing 70% H_2O for times of (a) 2 min, (b) 26 h, and (c) 47 h after solution preparation.

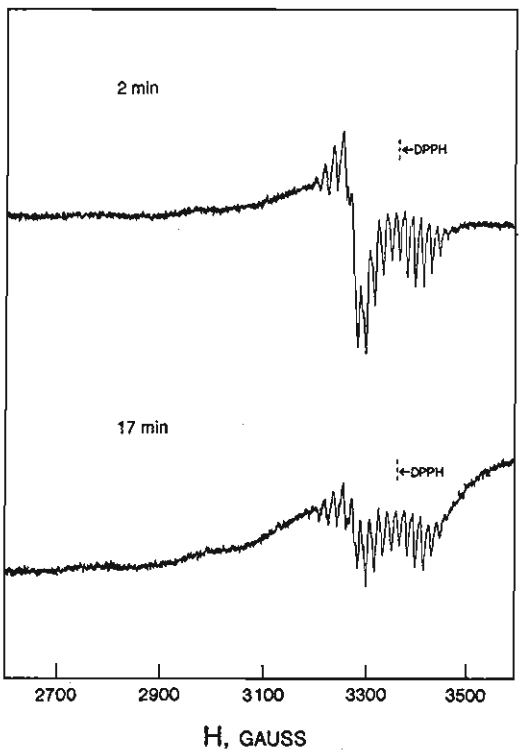

Figure 10. Time-dependent ESR spectra for 5.6×10^{-5} M $[(hTripP)Cu]^+$ at 134 K in an EtOH–H_2O solution containing 60% H_2O. The two solutions were held at room temperature for 2 and 17 min prior to freezing in liquid nitrogen.

Clearly, the ESR signal in Figure 8d cannot be assigned as due to a simple dimer.

The solution composition in which the ESR spectrum begins to change with increasing H_2O concentration is similar to the solution composition where the UV–visible spectra also begin to change under the same experimental conditions. The UV–vis data were interpreted in terms of micelle formation, and this assignment is consistent with the ESR data, which suggest that the signal in

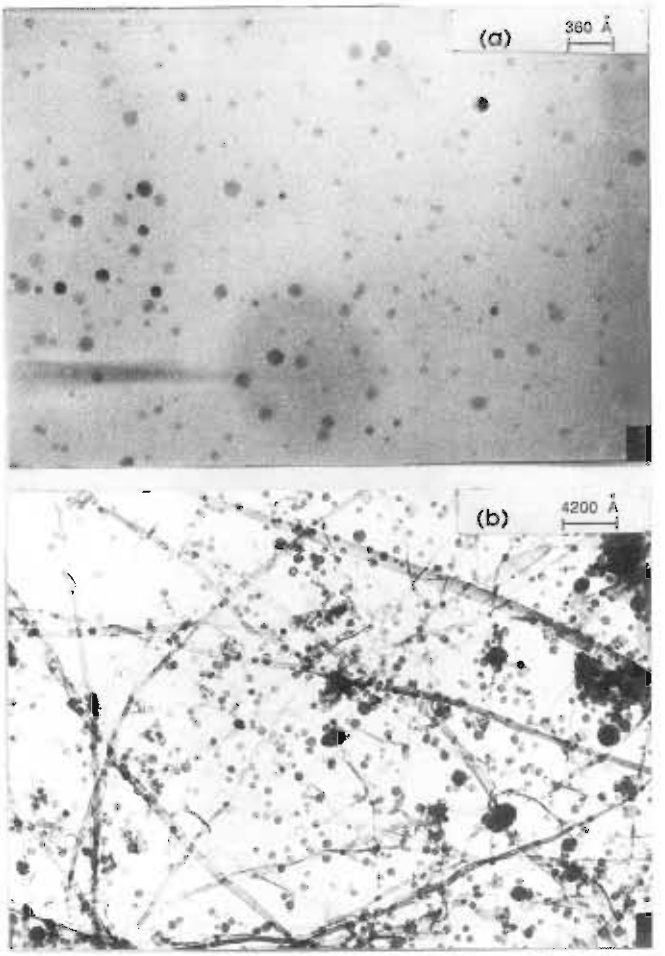

Figure 11. Electron micrographs of $[(hTriP)Ni]^+$ in an EtOH–H_2O mixture with 80% H_2O.

Figure 8c is due to overlapped spectra of a monomeric and micellized porphyrin complex. The ESR data also suggest that micelles are substantially formed in solutions containing 60% H_2O and that an optimum micellization is observed in the 65–80% H_2O region. Only a weak monomeric ESR signal is observed in solutions containing 90% H_2O.

Monomeric ESR spectra of $[(hTriP)VO]^+$ are obtained at 123 K in pure EtOH as well as in all EtOH–H_2O solutions containing 0–90% H_2O. This contrasts with the ESR results for $[(hTriP)Cu]^+$, which are discussed above, and is consistent with differences in the UV–visible spectra of the two complexes in solutions of 70% H_2O. These latter data show that the decrease in Soret band absorbance is less for $[(hTriP)VO]^+$ than for $[(hTriP)Cu]^+$ under the same solution conditions, and this can be attributed to a noninteraction of the paramagnetic centers in the former complex (which could result from trans coordination to the vanadium atom) or alternatively to a slow aggregation process.

A broad signal with $\Delta H = 37$ G appears at $g = 1.98$ when a water-containing solution of $[(hTriP)VO]^+$ is left at room temperature for periods longer than 20 h. This is shown in Figure 9, which illustrates the spectra obtained at 26 and 47 h after solution preparation. The signal at $g = 1.98$ gradually increases in intensity from 2 min to 47 h, and at the same time, the signals of the monomeric VO complex become weaker as micelles are formed. The signal at $g = 1.98$ is shaded in Figure 9b,c and is attributed to the micellar form of the porphyrin.

The time-dependent ESR signals of $[(hTriP)Cu]^+$ were also monitored at various times before freezing with liquid nitrogen. The broad ESR signal of the micellized porphyrin in a solution of 60–65% H_2O decreases with time and the initially broad signal almost totally disappears after 17 min, as shown in Figure 10. The ESR spectrum of $[(hTriP)Cu]^+$ in solutions of 90% H_2O (Figure 8e) does not have a micelle component signal, and these

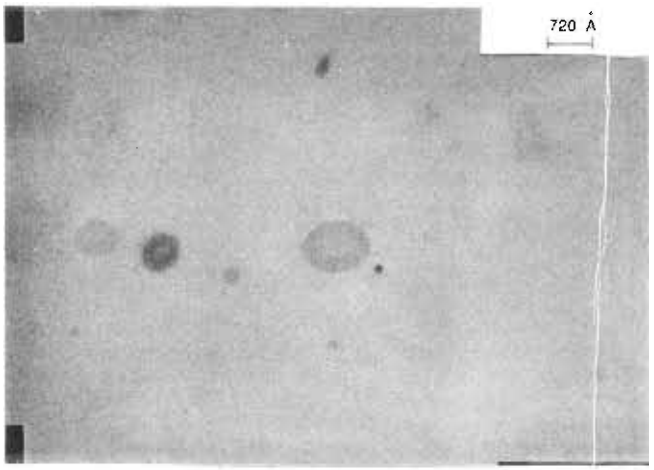

Figure 12. Electron micrograph of $[(hTriP)Cu]^+$ in an EtOH–H_2O solution with 80% H_2O.

solutions are clear, indicating that no precipitation has occurred. The signal due to the monomer is also weaker under these experimental conditions than in pure EtOH, and this suggests the formation of larger aggregates in solution.

In summary, the disappearance of the broad ESR signal in Figure 10 and the decrease of intensity in the UV–visible bands in Figures 4 and 5, as well as the precipitation of the porphyrin in EtOH–H_2O solutions with 60–70% H_2O, all indicate that the micellized porphyrins exist as large colloids that precipitate out of solution. This is related to further aggregation of the micellized porphyrins, which were further characterized by electron microscopy data.

Electron Microscopy. Electron microscopy has been used to study micelle formation[38-43] and will give the size of the micelle in a given solution. This technique was utilized for $[(hTrip)Ni]^+$ and $[(hTrip)Cu]^+$ in an EtOH–H_2O mixture with 80% H_2O, and the resulting photograph obtained for $[(hTriP)Ni]^+$ is reproduced in Figure 11a. As seen in this photograph, the diameter of the spherical micelles varies between 50 and 120 Å. Large spherical particles (with diameters varying between 500 and 1000 Å) are seen upon enlargement of the photograph, and cylindrical fibers with identical diameters are also observed. The presence of both large spherical particles and fibers is consistent with the micellar solution decomposing via an aggregation of regular micelles. This is illustrated in Figure 11b, which clearly shows the formation of fibers.

The electron microscopy data for $[(hTriP)Cu]^+$ do not permit a detection of regular spherical micelles with diameters of 50–100 Å, but several particles between 500 and 900 Å are observed (see Figure 12). This result clearly demonstrates that micellar solutions of $[(hTriP)Cu]^+$ tend to aggregate more than micellar solutions of $[(hTriP)Ni]^+$. Moreover, it is remarkable to note the circular images of ~70 Å diameter on the periphery of the micelle. These presumably correspond to regular micelles. Thus, all of the data are consistent with a spherical model that has the hydrophobic alkyl chains inside the cavity. The data are also consistent with a decomposition of the micelles via further aggregation.

Acknowledgment. The support of the National Science Foundation (Grants CHE-8515411 and INT-8413696), the CNRS, and Elf France is gratefully acknowledged. We thank Dr. P. Dufour from the Laboratoire de Reactivité des Solides (Dijon, France) for use of the electron microscopy apparatus.

(38) Imae, T.; Kamiya, R.; Ikeda, S. *J. Colloid Interface Sci.* **1984**, *99*, 300.
(39) Imae, T.; Kamiya, R.; Ikeda, S. *J. Colloid Interface Sci.* **1985**, *108*, 215.
(40) Murakami, Y.; Kikuchi, J.; Takaki, T.; Uchimura, K. *Bull. Chem. Soc. Jpn.* **1986**, *59*, 515.
(41) Bachmann, L.; Dasch, W.; Kutter, P. *Ber. Bunsen-Ges. Phys. Chem.* **1981**, *85*, 883.
(42) Murakami, Y.; Kikuchi, J.; Takaki, T.; Uchimura, K.; Nakano, A. *J. Am. Chem. Soc.* **1985**, *107*, 2161.
(43) Miller, D. D.; Bellare, J. R.; Evans, D. F.; Talman, Y.; Ninham, B. W. *J. Phys. Chem.* **1987**, *91*, 674.